Electronic Supplementary Information

Analytical figures of merit of a low-dispersion aerosol transport system for high-throughput LA-ICP-MS analysis

Thibaut Van Acker,*[a] Stijn J. M. Van Malderen,[b] Tom Van Helden,[a] Ciprian Stremtan,[b] Martin Šala,[c] Johannes T. van Elteren [c] and Frank Vanhaecke [a]

[a]*Atomic & Mass Spectrometry – A&MS Research Group, Department of Chemistry, Ghent University, Campus Sterre, Krijgslaan 281-S12, 9000 Ghent, Belgium*

[b]*Teledyne CETAC Technologies, 14306 Industrial Rd, Omaha, NE 68144, USA*

[c]*Department of Analytical Chemistry, National Institute of Chemistry, Hajdrihova 19, SI-1000 Ljubljana, Slovenia*

*Corresponding author, e-mail address: Thibaut.VanAcker@UGent.be, phone number: +32 9 264 4851.

Author contact information:

Thibaut Van Acker	Thibaut.VanAcker@UGent.be	ORCID: https://orcid.org/0000-0002-0649-7228
Stijn J. M. Van Malderen	Stijn.VanMalderen@Teledyne.com	ORCID: https://orcid.org/0000-0002-3879-7882
Tom Van Helden	Tom.VanHelden@UGent.be	ORCID: https://orcid.org/0000-0001-8728-7849
Ciprian Stremtan	Ciprian.Stremtan@Teledyne.com	ORCID: https://orcid.org/0000-0002-3308-738X
Martin Šala	Martin.Sala@ki.si	ORCID: https://orcid.org/0000-0001-7845-860X
Johannes T. van Elteren	Elteren@ki.si	ORCID: https://orcid.org/0000-0003-2237-7821
Frank Vanhaecke	Frank.Vanhaecke@UGent.be	ORCID: https://orcid.org/0000-0002-1884-3853

Electronic Supplementary Information

Table of contents

1. Tables

1.1. Table S1

Table S1. List of predicted average fluid velocities, Reynolds numbers and pressure drops for aerosol transport tubing of varying length and ID.

Length (m)	ID (mm)	v_{avg} (m s^{-1})	Re (-)	|ΔP| (mbar)
0.50	0.75	17.2	109	100
0.50	1.00	10.3	87	33
0.50	2.00	2.6	45	2
0.75	0.75	16.5	105	147
0.75	1.00	10.1	86	49
0.75	2.00	2.6	45	3
1.00	0.75	15.9	101	192
1.00	1.00	10.0	85	64
1.00	2.00	2.6	45	4
1.50	0.75	14.8	94	277
1.50	1.00	9.7	82	95
1.50	2.00	2.6	45	6
3.00	0.75	12.6	80	505
3.00	1.00	9.0	76	183
3.00	2.00	2.6	44	12

1.2. Table S2

Table S2. Instrument settings and data acquisition conditions for evaluating the influence of tubing ID, length and curvature on the analytical performance of aerosol transport systems.

Analyte G2 193 nm ArF*excimer-based LA-unit with HelEx-II ablation chamber					
	Standard ATS PTFE tubing 4 mm OD 2 mm ID 3 m length	**Standard ATS PTFE tubing 4 mm OD 2 mm ID 1 m length**	**Improved ATS PTFE tubing 2 mm OD 1.3 mm ID 0.75 m length**	**ARIS PEEK tubing 1/16" OD 0.04" ID 3 m length**	**ARIS PEEK tubing 1/16" OD 0.03" ID 0.9 m length**
Laser energy density (J cm^{-2})	3.5	3.5	3.5	3.5	3.5
Repetition rate (Hz)	1	5	10	1	5
Lateral scan speed (µm s^{-1})	20	100	200	20	50
Beam waist diameter (µm)	20	20	20	20	10
Dosage (shots $position^{-1}$)	1	1	1	1	1
He carrier gas flow rate (L min^{-1})	0.85	0.65	0.65	0.49	0.60
ICP-mass spectrometer	iCAP Q	XSeries-II	XSeries-II	iCAP Q	Agilent 7900
RF power (W)	1240	1350	1350	1240	1500
Ar plasma gas flow rate (L min^{-1})	14.0	13.0	13.0	14.0	15.0
Ar auxiliary gas flow rate (L min^{-1})	1.00	0.70	0.70	1.00	0.90
Ar make-up gas flow rate (L min^{-1})	0.70	0.69	0.69	0.70	1.02
Acquired m/z ratio (amu)	238	238	238	238	238
Respective dwell times (ms)	10	2	2	0.5	1
Total scan cycle time (ms)	10	2	2	0.5	1

1.3. Table S3

Table S3. Instrument settings and data acquisition conditions for evaluating the analytical performance of the ARIS and standard ATS in combination with a 2nd generation two-volume ablation cell.

Analyte G2 193 nm ArF*excimer-based LA-unit with HelEx-II ablation chamber		
	Standard ATS	**ARIS**
Laser energy density (J cm^{-2})	3.5	3.5
Repetition rate (Hz)	1	1
Lateral scan speed (µm s^{-1})	20	20
Beam waist diameter (µm)	20	20
Dosage (shots $position^{-1}$)	1	1
He carrier gas flow rate (L min^{-1})	0.85	0.49
Thermo iCAP Q ICP-mass spectrometer		
RF power (W)	1240	1240
Ar plasma gas flow rate (L min^{-1})	14.0	14.0
Ar auxiliary gas flow rate (L min^{-1})	1.00	1.00
Ar make-up gas flow rate (L min^{-1})	0.70	0.70
Acquired m/z ratio (amu)	238	238
Respective dwell times (ms)	10	0.5
Total scan cycle time (ms)	10	0.5

1.4. Table S4

Table S4. Instrument settings and data acquisition conditions for evaluating the analytical performance of the ARIS across a wide range of laser beam sizes.

Analyte G2 193 nm ArF*excimer-based LA-unit with HelEx-II ablation chamber + ARIS	
Laser energy density (J cm^{-2})	3.5
Repetition rate (Hz)	1
Lateral scan speed (µm s^{-1})	10-110
Beam waist diameter (µm)	10-110
Dosage (shots $position^{-1}$)	1
He carrier gas flow rate (L min^{-1})	0.6
Agilent 7900 ICP-mass spectrometer	
RF power (W)	1500
Ar plasma gas flow rate (L min^{-1})	15.0
Ar auxiliary gas flow rate (L min^{-1})	0.90
Ar make-up gas flow rate (L min^{-1})	1.00
Acquired m/z ratio (amu)	238
Respective dwell times (ms)	4
Total scan cycle time (ms)	4

1.5. Table S5

Table S5. Instrument settings and data acquisition conditions for evaluating the analytical performance of the ARIS in combination with a 3rd generation low-dispersion ablation cell.

Iridia 193 nm ArF*excimer-based LA-unit with Cobalt ablation chamber + ARIS	
Laser energy density (J cm^{-2})	4.0
Repetition rate (Hz)	50
Lateral scan speed (µm s^{-1})	250
Beam waist diameter (µm)	5
Dosage (shots $position^{-1}$)	1
He carrier gas flow rate (L min^{-1})	0.7
Agilent 7900 ICP-mass spectrometer	
RF power (W)	1500
Ar plasma gas flow rate (L min^{-1})	15.0
Ar auxiliary gas flow rate (L min^{-1})	0.90
Ar make-up gas flow rate (L min^{-1})	1.00
Acquired m/z ratio (amu)	238
Respective dwell times (ms)	0.1
Total scan cycle time (ms)	0.1

1.6. Table S6

Table S6. Instrument settings and data acquisition conditions for evaluating laser-induced elemental fractionation and oxide formation at high laser repetition rates

Iridia 193 nm ArF*excimer-based LA-unit with Cobalt ablation chamber + ARIS		
	U^+/Th^+ evaluation	**UO^+/U^+ evaluation**
Laser energy density (J cm^{-2})	4.0	4.0
Repetition rate (Hz)	50-1000	50-1000
Lateral scan speed (µm s^{-1})	12.5-250	12.5-250
Beam waist diameter (µm)	5	5
Dosage (shots $position^{-1}$)	20	20
He carrier gas flow rate (L min^{-1})	0.7	0.7
Agilent 7900 ICP-mass spectrometer		
RF power (W)	1500	1500
Ar plasma gas flow rate (L min^{-1})	15.0	15.0
Ar auxiliary gas flow rate (L min^{-1})	0.90	0.90
Ar make-up gas flow rate (L min^{-1})	1.00	1.00
Acquired m/z ratios (amu)	232 & 238	238 & 254
Respective dwell times (ms)	98 & 98	98 & 98
Total scan cycle time (ms)	200	200

1.7. Table S7

Table S7. Instrument settings and data acquisition conditions for evaluating the analytical performance of the ARIS and Cobalt ablation chamber across a wide range of laser repetition rates.

Iridia 193 nm ArF*excimer-based LA-unit with Cobalt ablation chamber + ARIS	
Laser energy density (J cm^{-2})	4.0
Repetition rate (Hz)	10-1000
Lateral scan speed (µm s^{-1})	2.5-250
Beam waist diameter (µm)	5 (square mask)
Dosage (shots $position^{-1}$)	1
He carrier gas flow rate (L min^{-1})	0.7
Agilent 7900 ICP-mass spectrometer	
RF power (W)	1500
Ar plasma gas flow rate (L min^{-1})	15.0
Ar auxiliary gas flow rate (L min^{-1})	0.90
Ar make-up gas flow rate (L min^{-1})	1.00
Acquired m/z ratio (amu)	238
Respective dwell times (ms)	0.1
Total scan cycle time (ms)	0.1

2. Figures

2.1. Figure S1

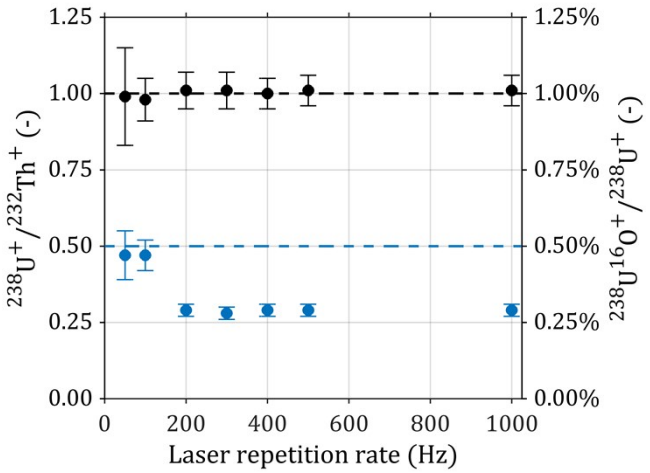

Figure S1. The average $^{238}U^{+}/^{232}Th^{+}$ (black circles) and $^{238}U^{16}O^{+}/^{238}U^{+}$ ratios (blue circles) with corresponding standard deviations obtained upon ablation of a NIST SRM 610 glass using a square spot size of 5 µm across the full range of laser repetition rates.